Electronic Supplementary Material (ESI) for Energy & Environmental Science.

Supplementary Information

Table of contents

Materials and Methods

Material preparation

The tetraethylene glycol dimethyl ether (TEGDME, ≥ 99%, Sigma-Aldrich) used as an organic solvent for the electrolyte was dried for more than 2 days with a molecular sieve (type 3Å, Sigma-Aldrich). Bis(trifluoromethane)sulfonimide lithium salt (LiTFSI, > 99.95%) was purchased from Sigma-Aldrich. It was dried for more than 2 days at 180 °C under vacuum. Benzoquinone derivatives, methyl-p-benzoquinone (98%), 2,5-dimethyl-1,4-benzoquinone (≥ 98%), duroquinone (97%), thymoquinone (≥ 98%), 2-tert-butyl-1,4-benzoquinone (98%), 2,5-di-tert-butyl-1,4-benzoquinone (99%), 2,6-di-tert-butyl-1,4-benzoquinone (98%), 2,5-di-tert-octyl-1,4-benzoquinone, and 2,5-dichloro-1,4-benzoquinone (98%) were purchased from Sigma-Aldrich and used as received. 2-Phenyl-1,4-benzoquinone (≥ 96%) and 2,3,5-trimethyl-1,4-benzoquinone (≥ 98%) were purchased from Tokyo Chemical Industry, and 2,5-di-phenyl-1,4-benzoquinone was purchased from Santa Cruz Biotechnology. The quinones were used as received. 1 M LiTFSI was dissolved in TEGDME solvent to produce a quinone-free electrolyte. The quinone-containing electrolytes were made by additionally dissolving 1 or 10 mM of each quinone. The final water content of all the electrolytes was confirmed to be less than 50 ppm by Karl Fischer titration. Before being used as an air electrode, the gas diffusion layer (H23, Freudenberg) was heat-treated at 900 °C for 3 h in an Ar:H_2 (95:5 volume ratio) atmosphere. A lithium iron phosphate (LFP) electrode was fabricated by coating slurry on Al foil. The slurry was prepared by mixing LFP powder, polyvinylidene fluoride, and super P with a weight ratio of 90:7:3 into 1-methyl-2-pyrrolidinone. Before being used as a separator, glass fiber (GF/D, Whatman) was washed with acetone and dried at 70 °C under vacuum for more than a day.

Lithium–oxygen cell assembly

A Swagelok-type cell was used to construct the lithium–oxygen cell. A sheet of gas diffusion layer was used as the air electrode. A sheet of glass fiber and a LFP electrode were used as the separator and counter electrode, respectively. The air electrode, separator, and counter electrode were prepared to have diameters of 1/2 inch. The amount of electrolyte used in assembling the cells was 200 μL. After cell assembly in an Ar-filled glove box (O_2 level < 0.1 ppm and H_2O level < 0.1 ppm), the atmosphere of the empty space above the air electrode was transformed to O_2 (> 99.999%), and the cells were operated as closed.

Electrochemical analysis and characterization

For the cyclic voltammetry experiment, a three-electrode beaker cell was used. A gold electrode and platinum wire were used as the working and counter electrode, respectively. For the reference electrode, 0.01 M Ag/Ag^+ in acetonitrile was used. For the linear sweep voltammetry analysis, a glassy carbon rotating disk electrode and rotating ring disk electrode with glassy carbon disk and Pt ring (PINE research) were used as the working electrodes, and the same counter and reference electrode as those used in the cycling voltammetry experiment were used. To rotate the electrodes, a rotator (PINE research, AFMSRCE) was employed. For the cyclic voltammetry and galvanostatic discharge experiments, a potentiostat (WonA Tech, WBCS 3000) was employed. For the linear sweep voltammetry experiment with a RDE and RRDE, a bi-potentiostat (Biologics, VSP-300) was employed. To calculate the diffusivity and heterogeneous electron transfer rate from the RDE profile, the kinematic viscosity was measured by a viscometer (Cannon–Fenske Routine Viscometer, Cannon Instrument Company). For observation of the electrode surface, field-emission scanning electron microscopy (SUPRA 55VP, Carl Zeiss) was used. The characterization of discharged electrode was conducted using X-ray diffraction (D2 phaser, Bruker).

Supplementary Figures

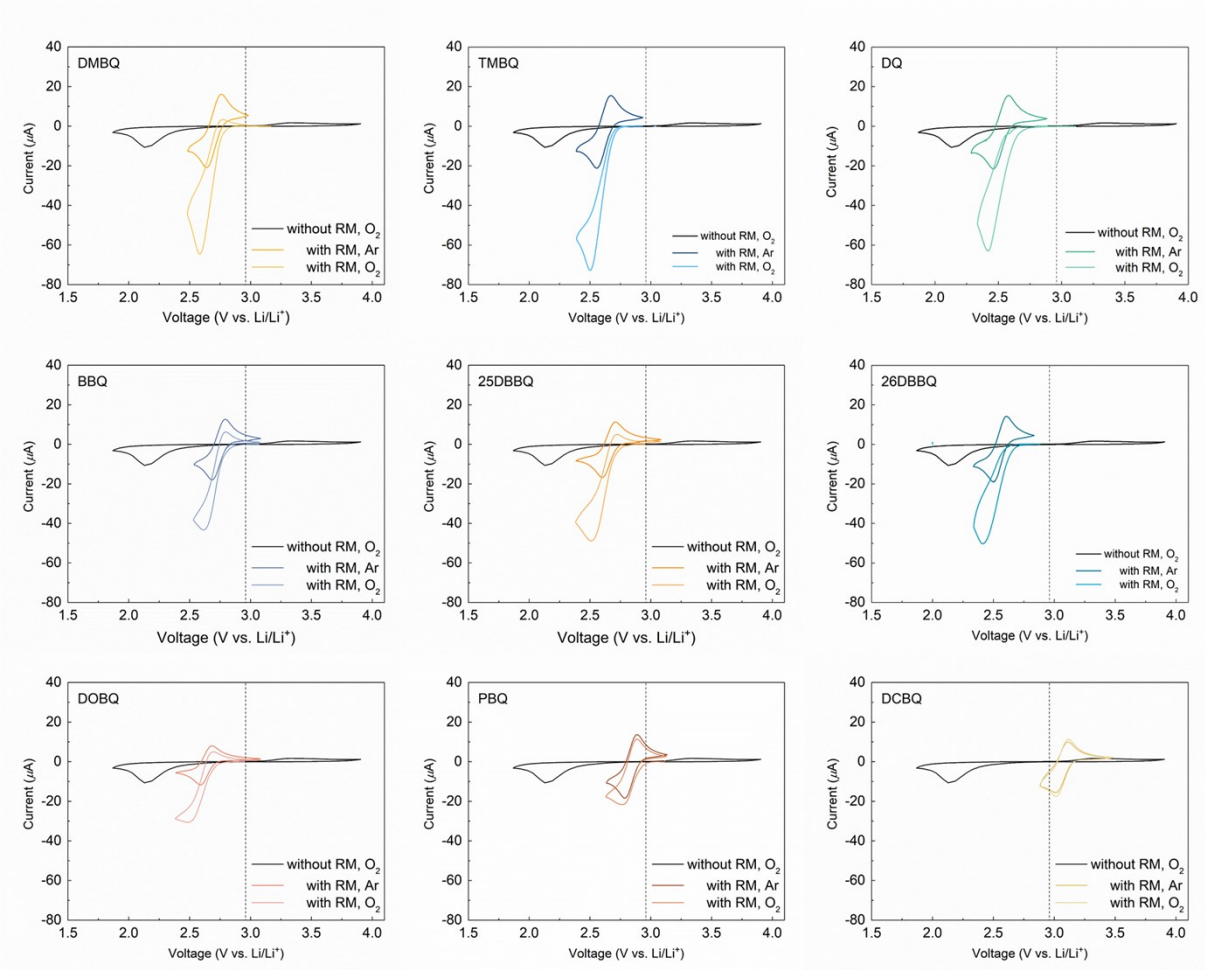

Figure S1. Cyclic voltammetry profiles of quinones. 1 M LiTFSI TEGDME with 10 mM of each quinone was used as an electrolyte and the scan rate of 50 mV s^{-1} were used to collect profiles.

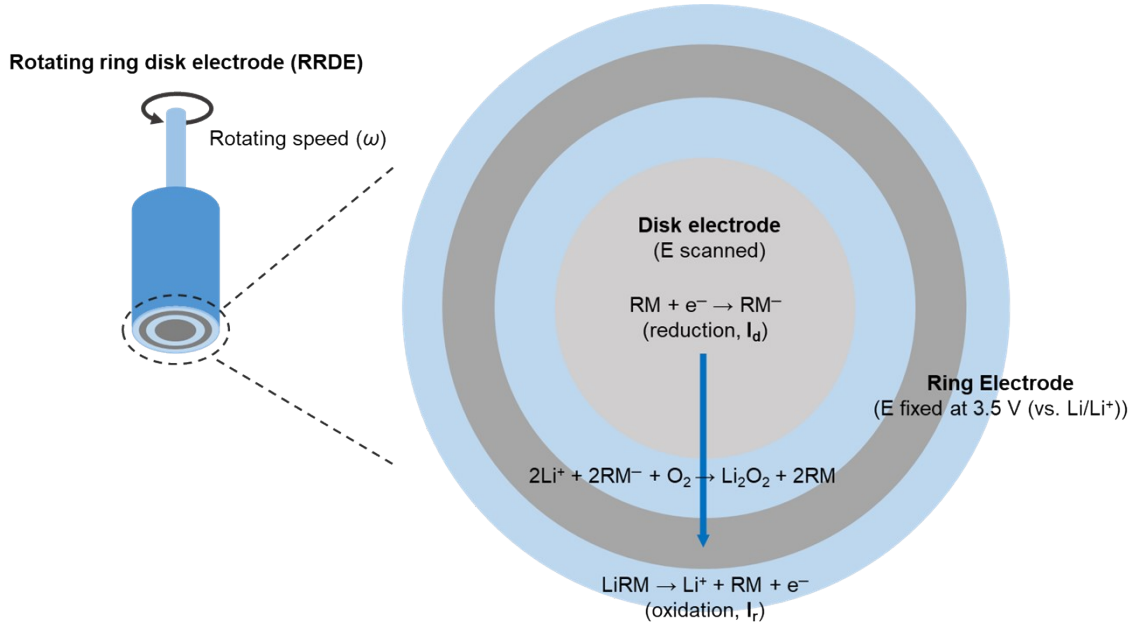

Figure S2. Schematics showing the reactions occurring at the rotating ring disk electrode (RRDE). At the disk electrode, RMs are reduced to generate disk current. Then they drift out to the ring electrode, where the reduced RMs are oxidized to generate ring current.

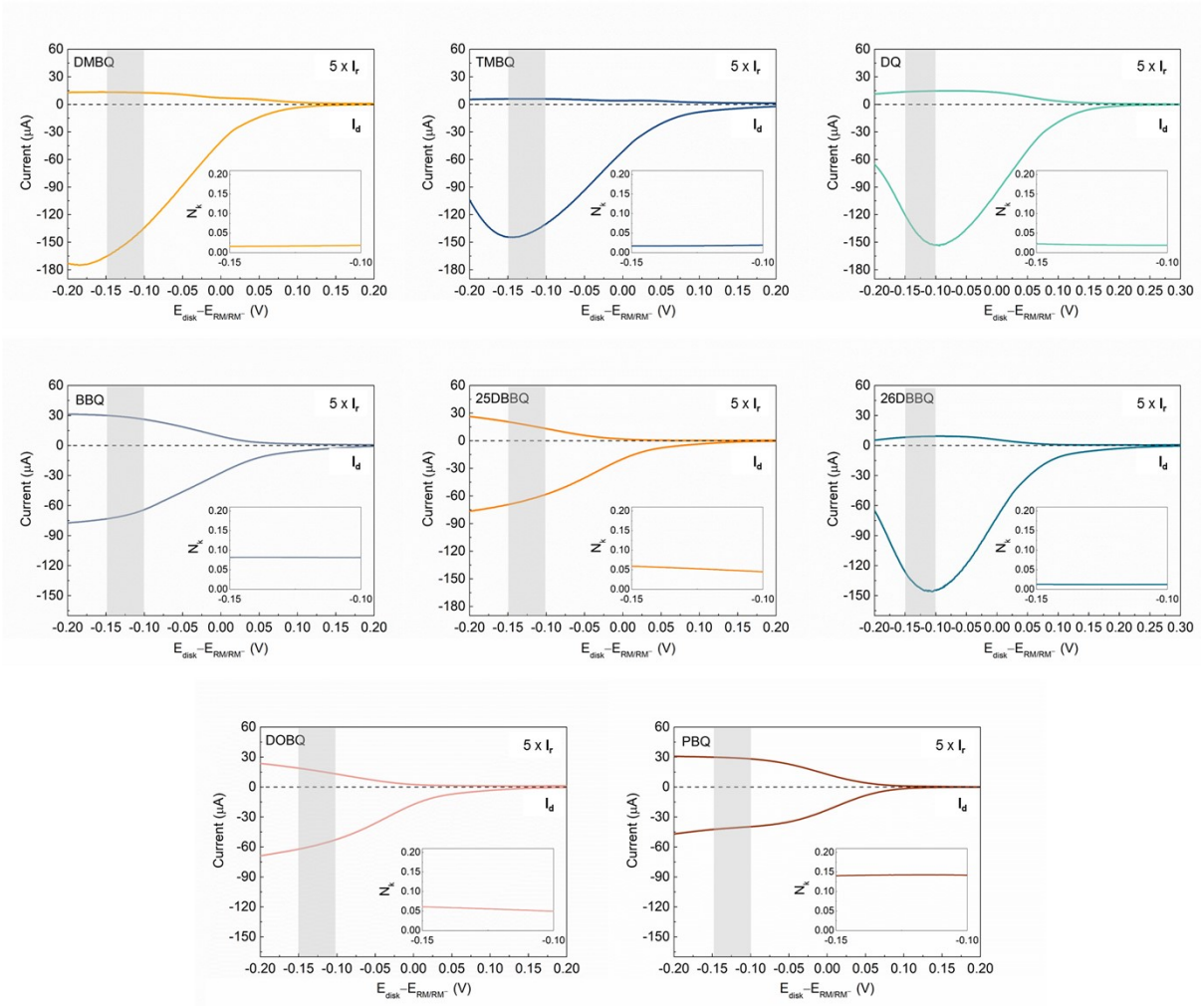

Figure S3. Linear sweep voltammetry profile with rotating ring disk electrode (RRDE). 1 M LiTFSI TEGDME containing 1 mM of each quinone was used as an electrolyte. The potential of disk electrode was scanned at the scan rate of 10 mV s^{-1}. Electrode was rotated with 2000 rpm. The ring current (I_r), disk current (I_d), and kinetic collection efficiency (N_k, I_r/I_d) are plotted.

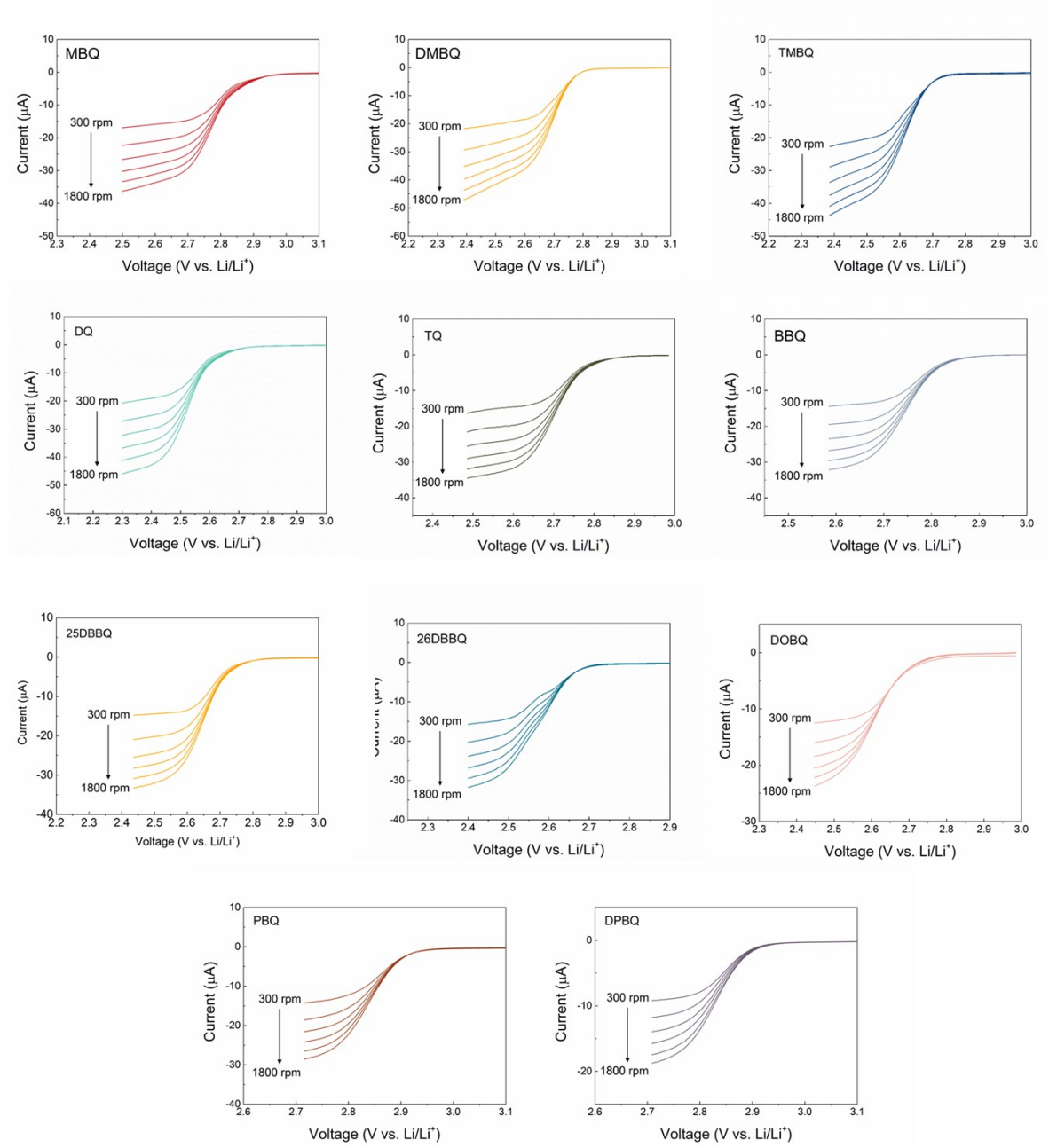

Figure S4. Linear sweep voltammetry profile with rotating disk electrode (RDE) at various rotating speeds from 300 rpm to 1800 rpm. 1 M LiTFSI TEGDME with 1 mM of quinone was used as an electrolyte and a scan rate of 10 mV s^{-1} were used.

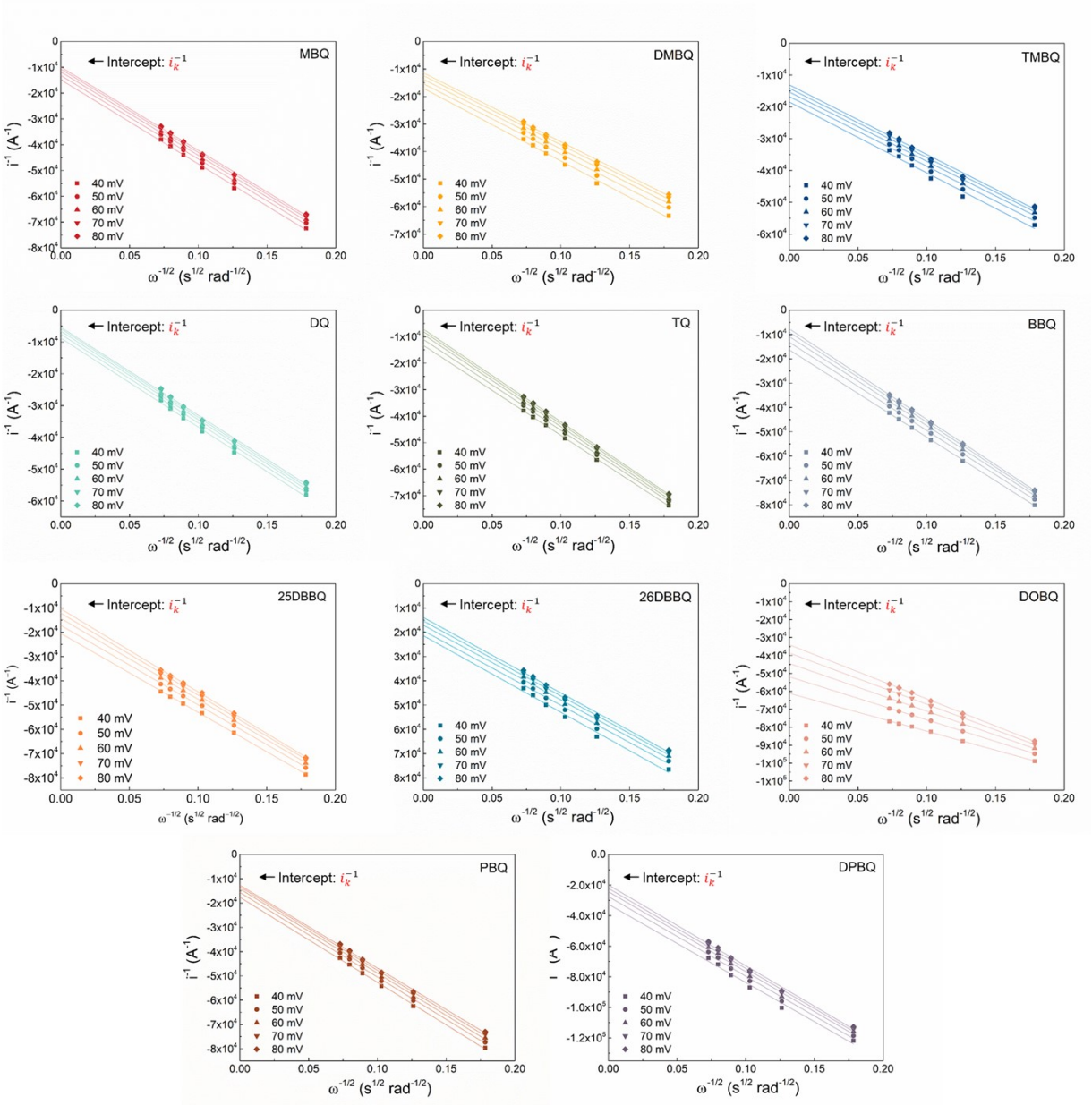

Figure S5. Plot of (rotating speed, ω)$^{-1/2}$ vs. (current, i)$^{-1}$ at various overpotentials and linear fitting lines whose y-intercept indicates i_k^{-1}.

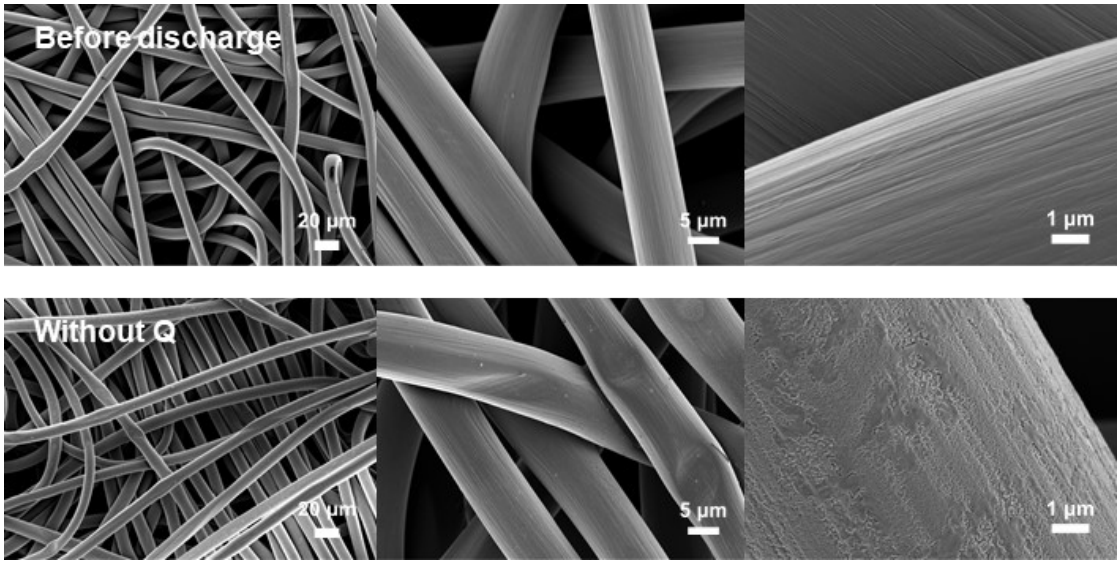

Figure S6. SEM images of electrode before (top) and after (bottom) discharge without a quinone. The surface of the electrode discharged without the quinone was passivated by a film-like discharge product.

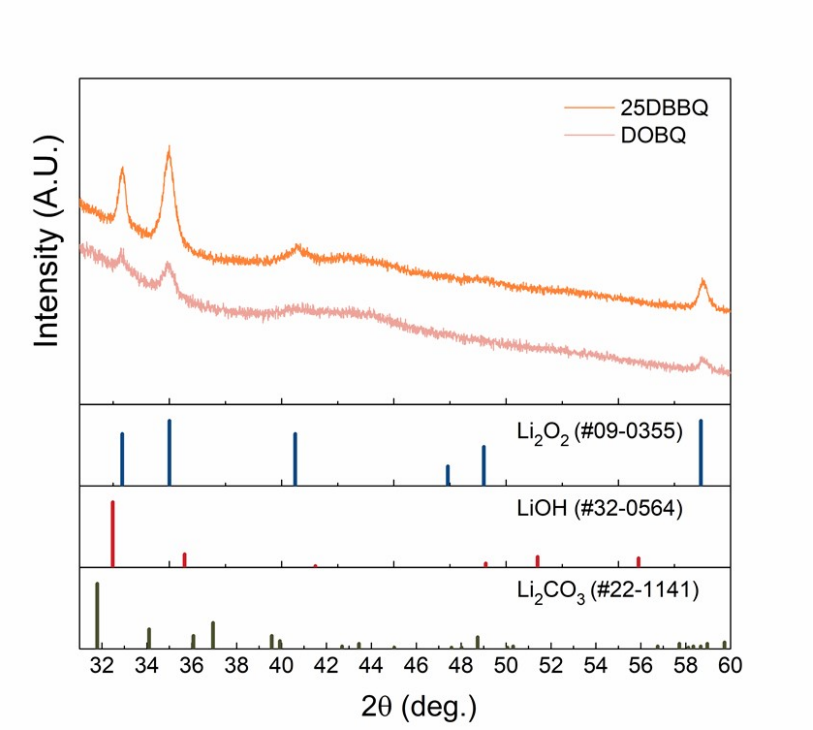

Figure S7. X-ray diffraction pattern collected from electrodes discharged with quinone-containing electrolytes confirming that the toroidal discharge product is lithium peroxide, Li_2O_2.

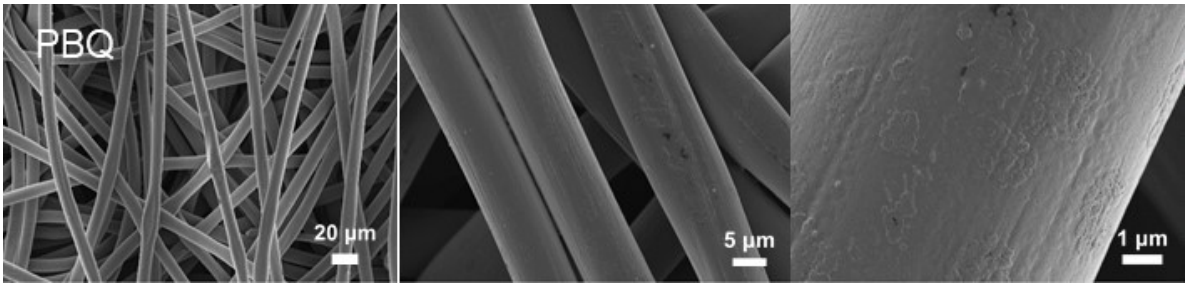

Figure S8. SEM images of electrodes discharged with PBQ. The low-magnification SEM images do not show much difference from the quinone-free case shown in figure S6. A higher magnification image shows that the formation of toroidal discharge products is limited leading to electrode passivation failing to achieve high discharge capacity.

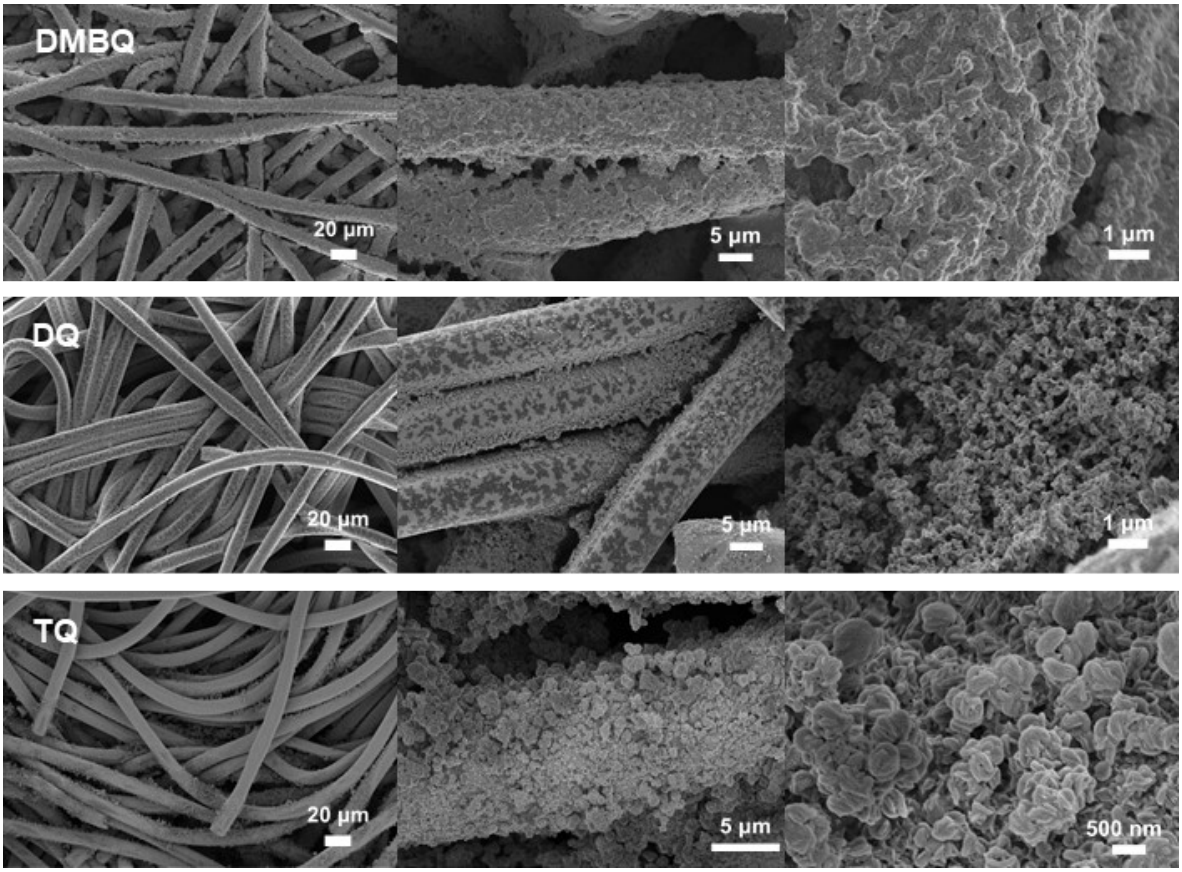

Figure S9. SEM images of electrodes discharged with quinones in group 3, DMBQ, DQ, and TQ. In all cases, the formation of the toroidal discharge product was observed, confirming catalytic effect of quinones. However, quinones also induce the passivation of electrode by toroidal discharge product, leading to limited discharge capacity.

Supplementary Tables

Table S1. Redox potential of quinones obtained from cyclic voltammetry.

Species	E_{RM/RM^-} (V vs. Li/Li^+)	Species	E_{RM/RM^-} (V vs. Li/Li^+)
MBQ	2.765	25DBBQ	2.658
DMBQ	2.698	26DBBQ	2.565
TMBQ	2.610	DOBQ	2.639
DQ	2.513	PBQ	2.832
TQ	2.696	DPBQ	2.830
BBQ	2.748	DCBQ	3.065

Table S2. Apparent rate constant for homogeneous electron transfer (k_{app}) calculated from RRDE experiment.

	Homogeneous electron transfer apparent rate constant, k_{app} (s^{-1})			Average	Standard deviation
Species	1st trial	2nd trial	3rd trial		
MBQ	0.196	0.187	0.187	0.190	0.00416
DMBQ	0.919	0.904	0.910	0.911	0.00609
TMBQ	1.149	1.168	1.173	1.163	0.0106
DQ	1.058	1.077	1.073	1.069	0.00810
TQ	0.930	0.921	0.915	0.922	0.00631
BBQ	0.503	0.497	0.485	0.495	0.00765
25DBBQ	0.772	0.647	0.710	0.710	0.0508
26DBBQ	1.024	1.025	1.028	1.026	0.00176
DOBQ	0.592	0.405	0.499	0.461	0.0929
PBQ	0.0133	0.0648	0.0109	0.0297	0.0249
DPBQ	0.039	0.062	0.018	0.040	0.0179

Table S3. Diffusivity of quinones calculated from rotating disk electrode (RDE) experiment.

	Diffusivity (cm^2 s^{-1})			Average	Standard deviation
Species	1st trial	2nd trial	3rd trial		
MBQ	2.72E-06	2.82E-06	2.66E-06	2.74E-06	6.82E-08
DMBQ	1.12E-06	1.16E-06	1.49E-06	1.26E-06	1.66E-07
TMBQ	1.78E-06	1.74E-06	1.69E-06	1.74E-06	3.82E-08
DQ	1.65E-06	1.67E-06	1.91E-06	1.74E-06	1.16E-07
TQ	1.38E-06	1.46E-06	1.26E-06	1.36E-06	8.16E-08
BBQ	1.54E-06	1.57E-06	1.59E-06	1.57E-06	2.32E-08
25DBBQ	1.35E-06	1.42E-06	1.40E-06	1.39E-06	2.82E-08
26DBBQ	1.24E-06	1.30E-06	1.30E-06	1.28E-06	2.56E-08
DOBQ	9.14E-07	9.33E-07	9.74E-07	9.40E-07	2.53E-08
PBQ	1.62E-06	1.54E-06	1.48E-06	1.55E-06	5.71E-08
DPBQ	7.80E-07	7.37E-07	9.08E-07	8.09E-07	7.28E-08

Table S4. Heterogeneous electron transfer rate constant for quinones calculated from the rotating disk electrode (RDE) experiment.

	Heterogeneous electron transfer rate constant, k_0 (cm s^{-1})			Average	Standard deviation
Species	1st trial	2nd trial	3rd trial		
MBQ	3.82E-03	3.92E-03	3.73E-03	3.82E-03	8.13E-05
DMBQ	3.63E-03	3.87E-03	4.68E-03	4.06E-03	4.51E-04
TMBQ	3.48E-03	3.67E-03	3.71E-03	3.62E-03	1.01E-04
DQ	4.71E-03	5.23E-03	7.20E-03	5.71E-03	1.07E-04
TQ	3.60E-03	4.07E-03	3.76E-03	3.81E-03	1.94E-04
BBQ	3.43E-03	2.95E-03	2.55E-03	2.98E-03	3.58E-04
25DBBQ	1.90E-03	1.64E-03	1.57E-03	1.70E-03	1.42E-04
26DBBQ	2.98E-03	3.53E-03	3.70E-03	3.41E-03	3.05E-04
DOBQ	1.31E-03	1.30E-03	1.31E-03	1.31E-03	3.71E-06
PBQ	5.07E-03	4.82E-03	4.27E-03	4.72E-03	3.37E-04
DPBQ	1.83E-03	1.78E-03	2.02E-03	1.88E-03	1.07E-04

Table S5. Discharge capacity from lithium-oxygen cells discharged with quinone-containing electrolytes

Species	Discharge capacity (mAh cm^{-2})			Average capacity (mAh cm^{-2})	Standard deviation
	1st trial	2nd trial	3rd trial		
MBQ	0.098	0.0786	0.0702	0.0823	0.01173
DMBQ	0.599	0.625	0.693	0.639	0.03972
TMBQ	0.688	0.809	0.664	0.720	0.06367
DQ	0.793	0.809	0.793	0.798	0.00764
TQ	0.776	0.849	0.977	0.867	0.08308
BBQ	0.421	0.407	0.351	0.393	0.03034
25DBBQ	2.565	2.585	2.815	2.655	0.11343
26DBBQ	0.984	0.595	0.589	0.723	0.18481
DOBQ	1.507	1.729	1.715	1.651	0.10142
PBQ	0.0484	0.0449	0.0533	0.0489	0.00345
DPBQ	0.0291	0.0362	0.0281	0.0312	0.00359

Supplemental note

Supplement note 1. Collection efficiency of rotating ring disk electrode experiment

On experiment using rotating ring disk electrode, a redox active species is reduced (oxidized) at disk electrode generating disk current, I_d. Then, a reduced (oxidized) species drifts out to the ring current and oxidized (reduced) to generate ring current, I_r. By calculating I_r/I_d, we can quantify the amount of species that is collected at a ring electrode after reacting at a disk electrode. If a reduced (oxidized) species is stable in electrolyte and does not change during diffusion from a disk to a ring, the collection efficiency is only the function of geometric factors of an electrode such as the radius of disk electrode, inner/outer diameter of ring electrode, and gap between two electrodes. Then, we can define theoretical collection efficiency ($N_{theoretical}$) that does not change with fixed electrode. $N_{theoretical}$ of the electrode used in the study was measured using a quinone species under Ar atmosphere. As shown in figure SN1, measure $N_{theoretical}$ is 0.144. If reduced species is reactive in electrolyte so that its amount reduces during drifting from a disk to a ring, collection efficiency is measured lower than $N_{theoretical}$ and it is defined as kinetic collection efficiency, N_k.

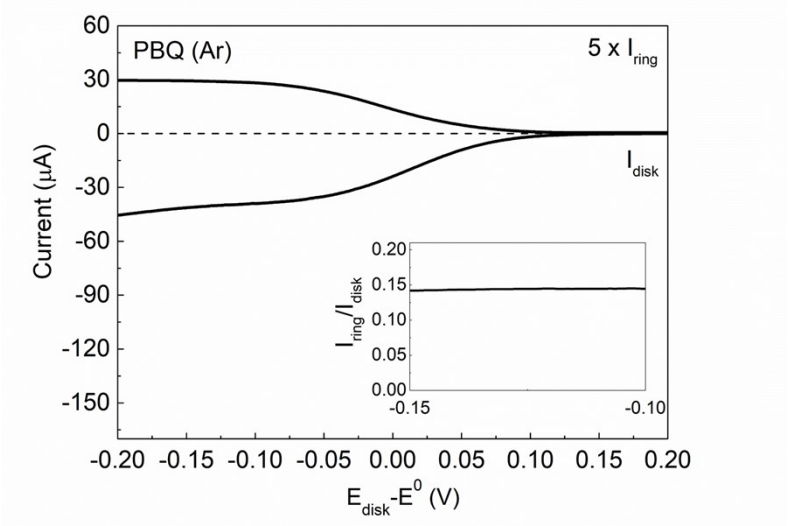

Figure SN1. Linear sweep voltammetry profile with rotating ring disk electrode (RRDE). 1 M LiTFSI TEGDME containing 1 mM of PBQ was used as the electrolyte and a scan rate of 10 mV s^{-1} were used. Electrode was rotated with 2000 rpm. $N_{theoretical}$, I_{ring}/I_{disk} was measured to be 0.144.

Supplement note 2. Measurement of diffusivity and heterogeneous electron transfer rate constant using rotating disk electrode

The current collected from the linear sweep voltammetry with rotating disk electrodes is expressed as follows according to the Koutecky–Levich equation:

$$\frac{1}{i}=\frac{1}{i_k}+\frac{1}{i_L}. \quad \text{- equation 1 (Koutecky–Levich equation)}$$

Here, i is the total current, i_k is the kinetic current, and i_L is the limiting current. According to the equation, when the overpotential is large enough to induce sufficiently high i_k to make the $\frac{1}{i_k}$ term assumed to be zero, i remains unchanged and equals i_L. Therefore, we can obtain i_L from a linear sweep voltammetry profile in the high overpotential region. Subsequently, i_L is expressed by the Levich equation as follows:

$$i_L = 0.62nFAD^{2/3}\omega^{1/2}\upsilon^{-1/6}C_0. \text{ – equation 2 (Levich equation)}$$

Here, *n* is the number of electrons during the redox reaction, *F* is the Faraday constant, A is the area of the electrode, D is the diffusivity, ω is the rotating speed, υ is the kinematic viscosity, and C_0 is the concentration of the redox active species. Here, the plot of $\omega^{1/2}$ *vs.* i_L with various rotating speeds shows a linear relationship with the slope of $0.62nFAD^{2/3}\upsilon^{-1/6}C_0$, which enables calculation of the diffusivity (*D*).

Combining equation 1 and 2 yields the following equation:

$$\frac{1}{i}=\frac{1}{i_k}+\frac{1}{0.62nFAD^{2/3}\omega^{1/2}\upsilon^{-1/6}C_0}. \text{ – equation 3}$$

According to equation 3, the plot of $\frac{1}{i}$ *vs.* $\omega^{-1/2}$ follows a linear relationship, yielding a fitting line with a y-intercept of $\frac{1}{i_k}$. Once we calculate i_k at various overpotentials, we can calculate i_0, the exchange current, by drawing a well-known Tafel plot. Finally, i_0 can be converted into the heterogeneous electron transfer rate constant (k_0) using the following simple equation:

$$i_0 = nFAk_0C_0$$ – equation 4

Figure S4 presents linear sweep voltammetry profile of all quinones studied here under various rotating speeds. According to the Levich equation, the plot of (rotating speed, ω)$^{1/2}$ *vs.* (limiting current, i_L) has a linear relationship with a slope related to the diffusivity. Plots of ω $^{1/2}$ *vs.* i_L and linear fitting lines for all the quinones are presented in Figure SN2a.

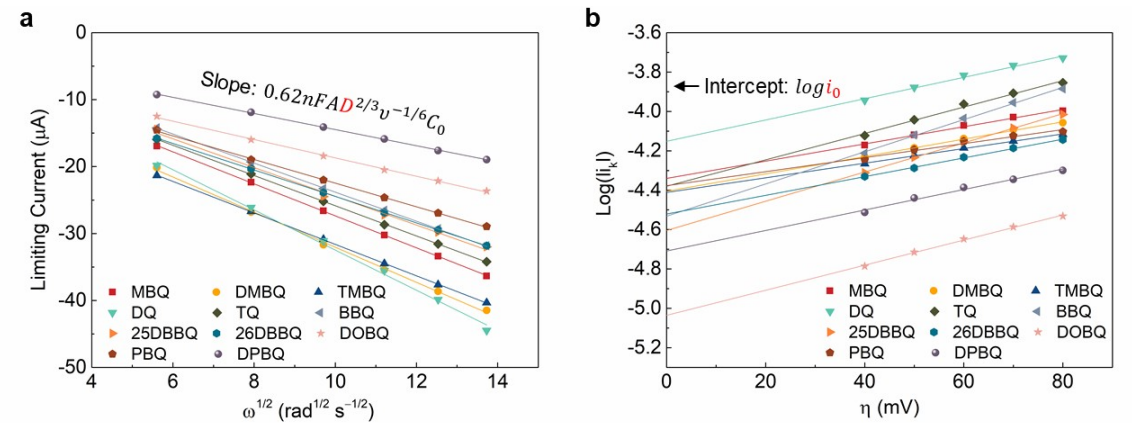

Figure SN2. a. Plot of (rotating speed)$^{1/2}$ vs. limiting current and linear fitting line. The diffusivity can be calculated from the slope of the fitting line, b. Plot of overpotential vs. log(i_k) and linear fitting line whose *y*-intercept indicates log(i_0).

The diffusivity for each quinone was calculated from the slope of the fitting line, and the values are listed in Table S3. The variables used to calculate diffusivity are as follows: A is 0.196 cm^2, υ is 0.1 cm^2 s^{-1}, and C_0 is 1 mM. The other kinetic parameter, k_0, was also measured using the Koutecky–Levich equation. According to this equation, the kinetic current (i_k) is given by the y-intercept of a linear fitting line of the plot of ω $^{-1/2}$ vs. i^{-1}. Figure S5 presents a plot of $\omega^{-1/2}$ vs. i^{-1} at various overpotentials (η) for all quinones. Finally, we calculated k_0 as the y-intercept of the linear fitting in the Tafel plot (η vs. log(i_k)), as shown in Figure SN2b. The calculated k_0 values are listed in Table S4.